

Improved Hematopoietic Differentiation Efficiency of Gene-Corrected Beta-Thalassemia Induced Pluripotent Stem Cells by CRISPR/Cas9 System

Bing Song,* Yong Fan,* Wenyin He, Detu Zhu,** Xiaohua Niu, Ding Wang, Zhanhui Ou, Min Luo, and Xiaofang Sun

The generation of beta-thalassemia (β -Thal) patient-specific induced pluripotent stem cells (iPSCs), subsequent homologous recombination-based gene correction of disease-causing mutations/deletions in the β -globin gene (*HBB*), and their derived hematopoietic stem cell (HSC) transplantation offers an ideal therapeutic solution for treating this disease. However, the hematopoietic differentiation efficiency of gene-corrected β -Thal iPSCs has not been well evaluated in the previous studies. In this study, we used the latest gene-editing tool, clustered regularly interspaced short palindromic repeats (CRISPR)/CRISPR-associated 9 (Cas9), to correct β -Thal iPSCs; gene-corrected cells exhibit normal karyotypes and full pluripotency as human embryonic stem cells (hESCs) showed no off-targeting effects. Then, we evaluated the differentiation efficiency of the gene-corrected β -Thal iPSCs. We found that during hematopoietic differentiation, gene-corrected β -Thal iPSCs showed an increased embryoid body ratio and various hematopoietic progenitor cell percentages. More importantly, the gene-corrected β -Thal iPSC lines restored *HBB* expression and reduced reactive oxygen species production compared with the uncorrected group. Our study suggested that hematopoietic differentiation efficiency of β -Thal iPSCs was greatly improved once corrected by the CRISPR/Cas9 system, and the information gained from our study would greatly promote the clinical application of β -Thal iPSC-derived HSCs in transplantation.

Introduction

BETA-THALASSEMIA (β -THAL), an inherited disorder caused by point mutations or small deletions in the β -globin gene (*HBB*), presented with the total absence or quantitative reduction in globin chain synthesis [1], and finally lead to moderate/severe anemia [2]. It is estimated that 4.5% of the population in the world carry β -Thal mutants [3]. More importantly, this inherited disease, which is prevalent throughout the southern part of China, has threatened millions of people's lives for decades [4]. β^0 -Thal major (TM), also known as Cooley's anemia [5], is the most severe form of this disease and is characterized by ineffective erythropoiesis (IE) and accompanied by abnormal hematological indices, extramedullary hematopoiesis, and iron deposit [1,5–9]. Toxic α -globin aggregates induce enhanced apoptosis, reactive oxygen species (ROS) accumulation, and damaged RBC membrane, which are the main reasons for the IE, but the underlying mechanisms are not very clear [10,11]. Babies with the severe forms of β -Thal can now survive, but require much more medical intervention, resulting in a rising global

economical and healthcare burden [12]. By now, hematopoietic stem cell transplantation (HSCT) remains the only definitive cure currently available for patients with thalassemia and sickle cell anemia [2,13,14]. However, the application of HSCT is limited by the lack of a matched donor for most patients [15] and a high risk of graft rejection from sensitization to HLA antigens [13].

The generation of induced pluripotent stem cells (iPSCs) from the somatic cells of patients with subsequent homologous recombination-based gene correction has raised hopes for curing blood diseases caused by genetic mutations. Such an approach would avoid the problems of immune rejection responses and may be a potential alternative source of hematopoietic stem cells (HSCs). To date, several research teams have established β -Thal patient-specific iPSCs from fibroblasts [16,17] and amniotic fluid cells [3,18]. It has been proven that transcription activator-like effector nuclease (TALEN)-corrected β -Thal iPSC lines can be induced to differentiate into HSCs [18,19]. Moreover, the genetically corrected β -Thal iPS-derived HSCs improved hemoglobin production in irradiated severe combined immunodeficiency

Key Laboratory for Major Obstetric Diseases of Guangdong Province, Key Laboratory of Reproduction and Genetics of Guangdong Higher Education Institutes, The Third Affiliated Hospital of Guangzhou Medical University, Guangzhou City, People's Republic of China.

*These two authors contributed equally to this work.

**Current affiliation: Department of Biological Sciences, National University of Singapore, Singapore, Singapore.

mice through bone marrow transplantation [19]. The study by Hanna found that a humanized sickle cell anemia mouse model could be rescued by transplanting genetically corrected iPSC-derived HSCs [15]. However, the hematopoietic differentiation efficiency of gene-corrected β -Thal iPSCs has not been well evaluated.

Recently, the clustered regularly interspaced short palindromic repeats (CRISPR) system is proven to be a powerful tool for targeted genetic modification. In this system, the CRISPR-associated 9 (Cas9) nuclease is directed by a 20-nt synthetic single-guide RNA (sgRNA) and introduces double-strand breaks into the genome, which will greatly enhance genome targeting efficiency through the host's cellular DNA repair machinery [20]. Compared with the previous zinc finger nuclease (ZFN) and TALEN, the CRISPR/Cas9 system possesses several advantages: simple easy programming; fast, inexpensive construction; robustly efficient mutagenesis; and multiplexed genome editing [21]. It has been proven that the system had a low off-targeting generation incidence using whole-genome sequencing [22]. Recently, Xie et al. carried out seamless gene correction in β -Thal iPSCs using CRISPR/Cas9 combined with *piggyBac* [23]. However, the impact of these corrections mediated by CRISPR/Cas9 on the differentiation potential of iPSCs still needs further evaluation.

In this study, we modeled the pathogenesis of β -Thal in vitro using β -Thal iPSCs that had a CD17 (A-T) homozygous point mutation in *HBB* (abbreviated as iPS- β 17/17). This point mutation of iPS- β 17/17 was corrected by the CRISPR/Cas9 system and induced hematopoietic differentiation using the embryoid body (EB) hanging drop method [24]. We evaluated the EB formation ratio, percentages of various hematopoietic differentiated progenitor cells, hematopoiesis-related gene expression, the number and distribution of colony-forming cells (CFCs), ROS production, early-stage apoptosis, and proliferation/apoptosis-related genes. Our results demonstrate that β -Thal iPSCs had reduced hematopoietic differentiation ability, while gene-corrected β -Thal iPSCs showed improved ability and restored *HBB* expression. These results will greatly promote the future clinical application of β -Thal patient-specific iPSC-derived HSCs in HSCT.

Materials and Methods

Feeder-dependent culture of hESCs and iPSCs

Human embryonic stem cell (hESCs) line 10 (named FY-hES-10 or hES-10), which was used as a positive control, was established in the Key Laboratory for Major Obstetric Diseases of Guangdong Province, The Third Affiliated Hospital of Guangzhou Medical University [25]. iPS- β 17/17 was generated from a β -Thal patient who had a CD17 (A-T) homozygous point mutation in *HBB* using the STEMCAA lentiviral system in the same laboratory. hES-10 and iPS- β 17/17 cell lines were expanded on mitomycin C-treated primary mouse embryonic fibroblast cells in hESCs culture medium consisting of knockout Dulbecco's modified Eagle's medium (DMEM), 15% knockout serum replacement, 5% inactivated fetal bovine serum (FBS), 2 mM GlutaMAX™, 1% nonessential amino acids, 1% penicillin/streptomycin, 0.1 mM β -mercaptoethanol (β -ME; all from Gibco), and 10 ng/mL human bFGF (Peprotech). The cells were maintained at 37°C and 5% CO₂ in a 100% humidified atmosphere incubator

and were passaged using 1 mg/mL dispase (Gibco) every 5–7 days.

Feeder-independent culture of hESCs and iPSCs

hES-10 and iPS- β 17/17 cell lines were cultured in the mTeSR1/Matrigel feeder-independent culture system. hESC-qualified Matrigel Matrix (354277; Corning) was diluted 1:30 with ice-cold DMEM/F-12, and the solution was allowed to set for 1 h at room temperature (RT) before use. Immediately before passaging cells, the excess Matrigel solution was aspirated from the 35-mm dishes, and 2 mL of fresh mTeSR medium was added to each dish. In the course of cell passage, the dishes were first examined to determine the passaging ratio. Second, the spent medium was aspirated, the cells were rinsed once with phosphate-buffered saline (PBS), and then 1 mL of RT dispase (1 mg/mL) was added. The cells were incubated in the 37°C, 5% CO₂ incubator for 5–7 min. After incubation, the dispase was aspirated, the cells were rinsed once with PBS, and the appropriate volume of mTeSR1 medium to collect the cells (usually 2–3 mL/dish) was added to each 35-mm dish. The cells were incubated overnight to allow clones to attach. The culture medium was refreshed daily with 2 mL/dish until the next passage or harvest.

Donor vector and guide RNA construction

Based on the homologous recombination method, the targeting scheme is summarized in Fig. 1A. B003 plasmid vector was used as the backbone, which had a LoxP-flanked and a PKG-promoted hygromycin resistance cassette (HygR). To construct the donor vector, 5-kb left and 3-kb right homology arms located in the second intron (I2) of a healthy individual's *HBB* gene were amplified by polymerase chain reaction (PCR) and inserted into the donor. The completed plasmid was linearized by the *NotI* enzyme and used for gene targeting. The guide RNA (gRNA) used in this study was targeted at the second intron of the *HBB* gene, and the sequence was GAATAACAGTGATAATTTCT.

Cleavage activity testing

The cleavage activity of the CRISPR/Cas9 system was tested in 293T cells. Briefly, about 10⁶ cells were transfected with 5 μ g pCas9/sgRNA plasmid using Lipofectamine LTX (Invitrogen). About 72 h post-transfection, the genomic DNA was extracted. Short fragments flanking the second intron locus were amplified by PCR and subjected to T7E1 digestion for 1 h at 37°C. The digested fragments were separated in 2% agarose gels. The primers used are listed in Table 1 (P3/P4).

Gene targeting

iPS- β 17/17 cells were treated with 10 μ M ROCK inhibitor (Y-27632, SCM075; Millipore) for 2 h before electroporation, and then washed with PBS once and dissociated with StemPro Accutase (A1110501; Gibco). After dissociation, cells were rinsed with DMEM/F12 twice and filtered through a 100- μ m cell strainer, then collected by centrifugation at 100 g for 5 min. About 3–5 \times 10⁶ iPS- β 17/17 cells were electroporated with 10 μ g of linearized donor vector, 3.75 μ g gRNA, and 1.25 μ g hCas9 (3:1) in a total volume of

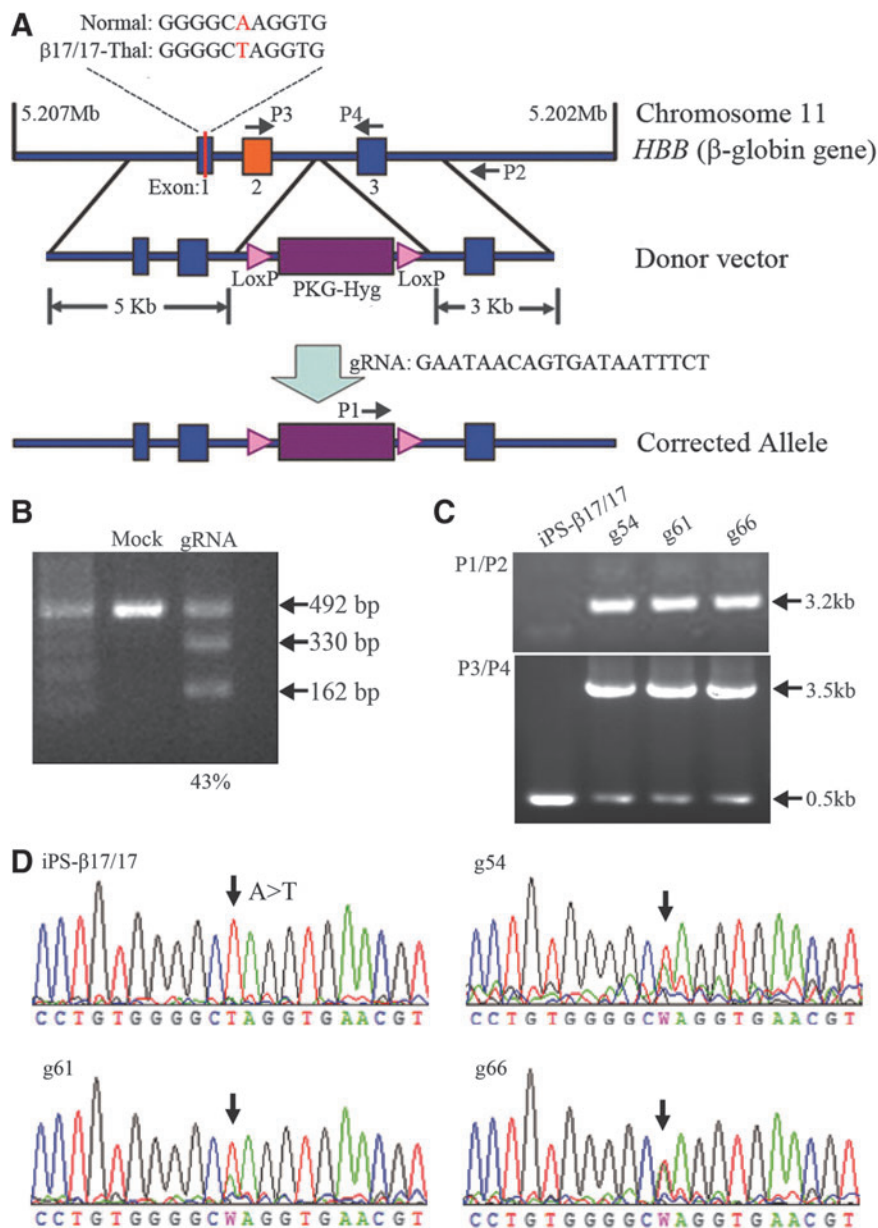


FIG. 1. Genetic correction of iPS- β 17/17 mutation by the CRISPR/Cas9 system. **(A)** Schematic representation of the gene-targeting strategy for correcting the (A \rightarrow T) point mutation in the *HBB* gene of iPS- β 17/17 cells using the CRISPR/Cas9 system. **(B)** Cleavage activity of the CRISPR system in 293T cells. The cleavage activity of the CRISPR/Cas9 system induced by gRNA was up to 43% using the T7E1 assay. **(C)** Identification of *HBB* gene-corrected clones using PCR analysis. The amplified target fragments, 3.2-kb by P1/P2, represented the HygR fragment integration into the 3' genomic DNA, while P3 and P4 were used to amplify 3.5- and 0.5-kb bands, which showed that the drug resistance cassette has integrated into the genomic DNA. **(D)** The sequencing results of the (A \rightarrow T) mutation site of the *HBB* gene in both iPS- β 17/17 and gene-corrected lines (g54, g61, and g66) using the Sanger method. If one of the alleles was successfully repaired, the peaks of A and T would be very close and shown as W. Cas9, CRISPR-associated 9; CRISPR, clustered regularly interspaced short palindromic repeats; gRNA, guide RNA; PCR, polymerase chain reaction.

300 μ L of PBS. The cells were exposed to a single 320 V, 200 μ F pulse at RT (time constant = 2.7–3.2 ms), and then plated onto a Matrigel-coated 10-cm dish in mTeSR1 supplemented with 10 μ M Y-27632 until small clones appeared (typically less than 48 h). Drug-resistant clones were selected by 50 μ g/mL hygromycin B (Sigma) for 2 weeks. The selected clones were verified by genomic PCR analysis and sequencing. The primer set used can be found in Table 1.

TABLE 1. PRIMER SETS USED IN IDENTIFYING GENE-CORRECTED CLONES

| | Sequence |
|----|-----------------------------------|
| P1 | 5'-CTG TAC AAC CAC CAT TTC ACT-3' |
| P2 | 5'-ATC TAA CAG CCA AGT CAA ATC-3' |
| P3 | 5'-CCT AGC TTG GAC TCA GAA T-3' |
| P4 | 5'-ACA GTC TGC CTA GTA CAT TAC-3' |

PCR analysis of *HBB* gene-corrected clones

If the targeted integration mediated by the homologous recombination successfully combined with the HygR and downstream of 3' homology arms, the primer set (P1 and P2, shown in Fig. 1A) will amplify a 3.2-kb product, or there will be no DNA production, while the primer set with P3 (on 5' homology) and P4 (on 3' homology arm) was used to amplify one 3.5- and one 0.5-kb product to identify the integration of drug resistance cassette into the genomic DNA (demonstrated in Fig. 1A). PCR analysis was performed using High Fidelity Platinum Taq (Invitrogen) according to the manufacturer's instructions, and about 100 ng genomic DNA templates were used in all reactions. The sequences of the two primer sets are shown in Table 1.

Hematopoietic differentiation in vitro

Efficient HSCs were generated from hESCs or iPSCs using a two-step differentiation strategy in combination with the EB

hanging drop method. Before hematopoietic differentiation, hES-10, iPS- β 17/17, and gene-corrected iPS- β 17/17 were treated with Accutase (Gibco) for 3 min to prepare single cells, and then suspended at a density of $2\text{--}4 \times 10^5$ cells per milliliter. First, 30 μ L EB drops containing the recombinant protein-based animal product-free medium, StemDiff APEL (StemCell Technologies), supplemented with 40 ng/mL human stem cell factor (SCF), 20 ng/mL bone morphogenetic protein 4 (BMP4), and 20 ng/mL vascular endothelial growth factor (VEGF; all from R&D Systems) were conducted for 4 days. Second, on day 5, EBs were harvested and plated into ultralow attachment plates. Four more cytokines, 20 ng/mL FMS-like tyrosine kinase receptor 3 ligand (FL), 20 ng/mL interleukin-6 (IL-6), 20 ng/mL thrombopoietin (TPO), and 20 ng/mL insulin-like growth factor II (IGF-II) were added to the StemDiff APEL medium, and the medium was changed every other day. After 14 days, EBs were harvested, washed once with PBS, and treated with TrypLE Select (Invitrogen) for 30 min in a 37°C water bath to prepare single-cell suspensions for further testing.

EB formation rate assessment

In the two-step EB hanging drop method to induce hematopoietic differentiation, we first counted the number of 30 μ L single-cell suspension drops as A. After 4 days, the formed EB drops, which were plated into ultralow attachment plates for further differentiation, were recorded as B, and the EB formation rate was calculated as $B/A \times 100\%$.

Hematopoietic differentiation efficiency assayed by flow cytometry

Single cells prepared from EBs were stained with the following fluorochrome-conjugated monoclonal antibodies (mAbs): phycoerythrin-cyanine7 (PE-Cy7)-labeled anti-human CD34, allophycocyanin (APC)-labeled anti-human CD45 and CD235a, and PE-labeled anti-human CD31 and CD71. These mAbs and their corresponding nonspecific isotype controls were used at 1 μ g/mL per 1×10^6 cells. The cells were stained with mAbs in PBS supplemented with 2% FBS for at least 30 min on ice. The cells were washed once with 2% FBS-PBS and resuspended with 300 μ L 2% FBS-PBS. Samples were tested using the Aria III flow cytometer (BD Biosciences) and analyzed with FACSDiva software (BD Biosciences). The polychromatic flow cytometry was performed with sorting CD34⁺ cells simultaneously, which were used in the colony-forming assay.

Colony-forming assay

On day 14, $\sim 5\text{--}10 \times 10^4$ single cells from sorted CD34⁺ cells during flow cytometry were plated into MethoCult H4434 (StemCell Technologies) and cultured for more than 2 weeks. Methylcellulose-based feed medium containing Iscove's modified Dulbecco's media (IMDM), 30% H4434, 0.75 mg/mL bovine serum albumin, 20% FBS, 2 mM GlutaMAX, 0.5 mM β -ME, $1 \times$ insulin-transferrin-sodium (ITS), 50 ng/mL SCF, 10 ng/mL IL-3, 10 ng/mL IL-6, 10 ng/mL granulocyte-macrophage colony-stimulating factor (GM-CSF), 6 U/ μ L EPO, and 1% penicillin/streptomycin was added every 3 days. Clones were imaged and scored according to their morphological criteria as erythroid (CFC-E), granulocyte/erythrocyte/macrophage/megakaryocyte (CFC-

GEMM), granulocyte/macrophage (CFC-GM), granulocyte (CFC-G), and macrophage (CFC-M).

ROS level detection by flow cytometry

ROS play a critical role in the cellular physiopathology. The 2',7'-dichlorodihydrofluorescein diacetate (H₂DCF-DA) fluorescent probe is commonly employed to detect ROS levels. This dye is a nonfluorescent reagent when chemically reduced. Upon oxidation by ROS and removing the acetate groups by cellular esterases, it will become fluorescent and can be detected by fluorescence microscopy and flow cytometry. Single cells were prepared as previously described and stained with the fluorochrome-conjugated mAbs, PE-Cy7-labeled anti-human CD34 and APC-labeled anti-human CD45. Then, cells were collected and washed once by cold PBS for 5 min. Two hundred microliters of H₂DCF-DA (10 μ M) was added to cells and incubated for 30 min at 37°C in the dark. Afterward, the ROS levels of CD34⁺/CD45⁺ cells were analyzed by a flow cytometer at FL1-A channel following the cell resuspension with 300 μ L 2% FBS-PBS. Samples were tested using the Aria III flow cytometer (BD Biosciences) and analyzed with FACSDiva software (BD Biosciences).

Early-stage apoptosis analyzed by Annexin-V staining

Apoptosis, a form of programmed cell death, could eliminate the cell number without releasing inflammatory mediators to the surrounding area. Annexin-V had a high affinity for membrane phosphatidylserine (PS) evagination at the early stage of apoptosis. Single cells and immunofluorescent staining of CD34⁺CD45⁺ HSCs were the same as above. Then, the cells were stained using the Apoptosis Detection Kit according to the instructions (556547; BD Pharmingen), and analyzed by a flow cytometer at FL1-A channel.

RNA extraction and real-time quantitative PCR analysis

Total RNA was extracted from day 14 EBs using TRIzol reagent (Invitrogen) according to the manufacturer's instructions. 1.5 μ g RNA was reverse transcribed to produce complementary DNA (cDNA) using the High-Capacity cDNA Reverse Transcription Kit (Applied Biosystems™). Real-time quantitative PCR (qPCR) was performed using a Platinum® SYBR® Green qPCR SuperMix-UDG with ROX Kit (Invitrogen). Data were analyzed using the StepOne™ software V2.2.2. *GAPDH* was used for quantitative reverse transcription PCR (qRT-PCR) normalization, and all items were measured in triplicate. The relative quantitative expression of the test gene was expressed as the ratio of the hematopoietic differentiated hESCs/iPSCs group and the undifferentiated hESCs/iPSCs group. The primer sequences used are listed in Table 2.

HBB and HBG protein tests using western blotting

On day 14, EBs from four groups were collected, washed once with cold PBS, and lysed in $1 \times$ cell lysis buffer (#9803; Cell Signaling) supplemented with 100 \times phenylmethanesulfonyl fluoride (PMSF, 100 mM) for 5 min. The lysate was centrifugated at 12,000 g for 10 min at 4°C to

TABLE 2. PRIMER SETS USED IN QUANTITATIVE REVERSE TRANSCRIPTION-POLYMERASE CHAIN REACTION

| Gene | Sequence-forward | Sequence-reverse |
|------------------|---|--------------------------------------|
| <i>FLK1</i> | 5'-CCA ACG AGA GGA GAG TCA TCG-3' | 5'-TTC CGT GTT GTA GAG GGT GGT-3' |
| <i>CD31</i> | 5'-ACC GTG ACG GAA TCC TTC TCT-3' | 5'-GCT GGA CTC CAC TTT GCA C-3' |
| <i>CD34</i> | 5'-TGC CCT GAG TCA ATT TCA CTT C-3' | 5'-CAA CTC TGT CTT GGC GTC AGT-3' |
| <i>CD45</i> | 5'-CTG AGT TTT GAA TGC CCT AAT G-3' | 5'-AAC AAT TTC CTC CTC TGT TAC CC-3' |
| <i>GATA-1</i> | 5'-CTG TCC CCA ATA GTG CTT ATG G-3' | 5'-GAA TAG GCT GCT GAA TTG AGG G-3' |
| <i>HBB</i> | 5'-TGC TCG GTG CCT TTA GTG ATG-3' | 5'-CCCAGGAGCCTGAAGTTCTCA-3' |
| <i>HBG</i> | 5'-GGG CAA GGT GAA TGT GGA AG-3' | 5'-AGG ACA GGT TGC CAA AGC TG-3' |
| <i>ITGA2B</i> | 5'-GAT GAG ACC CGA AAT GTA GGC-3' | 5'-GTC TTT TCT AGG ACG TTC CAG TG-3' |
| <i>KLF1</i> | 5'-GGT TGC GGC AAG AGC TAC A-3' | 5'-GTCAGAGCGCGAAAAAGCAC-3' |
| <i>RUNX1</i> | 5'-CTG CCC ATC GCT TTC AAG GT-3' | 5'-GCC GAG TAG TTT TCA TCA TTG CC-3' |
| <i>FOG1</i> | 5'-CGT GCT TCG AGT GCG AGA T-3' | 5'-GGC CTG AAC AGT AGA GGC G-3' |
| <i>Ki67</i> | 5'-CGA CCC TAC AGA GTG CTC AAC AA-3' | 5'-CTT GTC AAC TGC GGT TGC TCC TT-3' |
| <i>PCNA</i> | 5'-CCA CTC TCT TCA ACG GTG ACA CT-3' | 5'-CAT CCT CGA TCT TGG GAG CCA A-3' |
| <i>Caspase-3</i> | 5'-GAC AGA CAG TGG TGT TGA TGA TGA C-3' | 5'-GCA TGG CAC AAA GCG ACT GGA T-3' |
| <i>Bcl-2</i> | 5'-TCA ACC GGG AGA TGT CGC-3' | 5'-GGG CCG TAC AGT TCC ACA AA-3' |
| <i>GAPDH</i> | 5'-CCT TCA TTG ACC TCC ACT AC-3' | 5'-GTT GTC ATA CTT CTC ATG GTT-3' |

remove the insoluble components. Concentrations of the samples were detected using NanoDrop 2000, and 30 μ g of proteins per group was separated by 15% sodium dodecyl sulfate–polyacrylamide gel electrophoresis (SDS-PAGE) and transferred to a PVDF membrane. After that, the membrane was blocked with 5% nonfat milk in TBS containing 0.1% Tween-20 (TBS-T), incubated overnight with anti-HBB (AP11557b; Abgent), anti-hemoglobin gamma (HBG, ab137096; Abcam), and anti-GAPDH (AP7873b; Abgent) Ab 4°C. Then, a goat anti-rabbit IgG horseradish peroxidase-linked secondary antibody (LP1001a; Abgent) was incubated for 1 h at RT. Finally, the blots were visualized using an ECL detection Kit (23225; Thermo).

Statistical analysis

Experiments were performed thrice with each experimental group to verify that the data were repeatable. All data are expressed as average values \pm standard deviations. Statistical analysis was performed using the unpaired Student's test, and $P < 0.05$ was regarded as statistically significant.

Results

Specific targeting of the *HBB* gene using the RNA-guided Cas9 nuclease-mediated system

We sought to correct these disease-causing mutations in β -Thal iPSCs through in situ gene targeting using the CRISPR/Cas9 system (Fig. 1A). The cleavage activity of the CRISPR/Cas9 system induced by gRNA was up to 43% using the T7E1 assay (Fig. 1B). After gene targeting, 18 Hyg-resistant clones were picked and expanded in the iPSC culture medium. They were then verified by PCR for HygR fragment integration into the genomic DNA. According to the P1/P2 and P3/P4 amplification results, three clones (g54, g61, and g66) were identified as the positive clones (Fig. 1C). We further verified the positive clones by direct sequencing the first exon (E1) of *HBB*. If one of the alleles was successfully repaired, the peaks of A and T would be very close and shown as W. The sequencing results showed that g54, g61, and g66 were correctly repaired and the representative sequencing results are shown in Fig. 1D. So, the targeting efficiency was 16.67% (3/18).

Besides, to monitor the possible off-targeting efficiency introduced by Cas9, five potential off-target sites were analyzed by the T7E1 assay (Supplementary Tables S1 and S2; Supplementary Data are available online at www.liebertpub.com/scd). Compared with the *HBB* locus, none of the five regions showed off-target cleavage in the genome of gene-corrected iPS- β 17/17 (Supplementary Fig. S1).

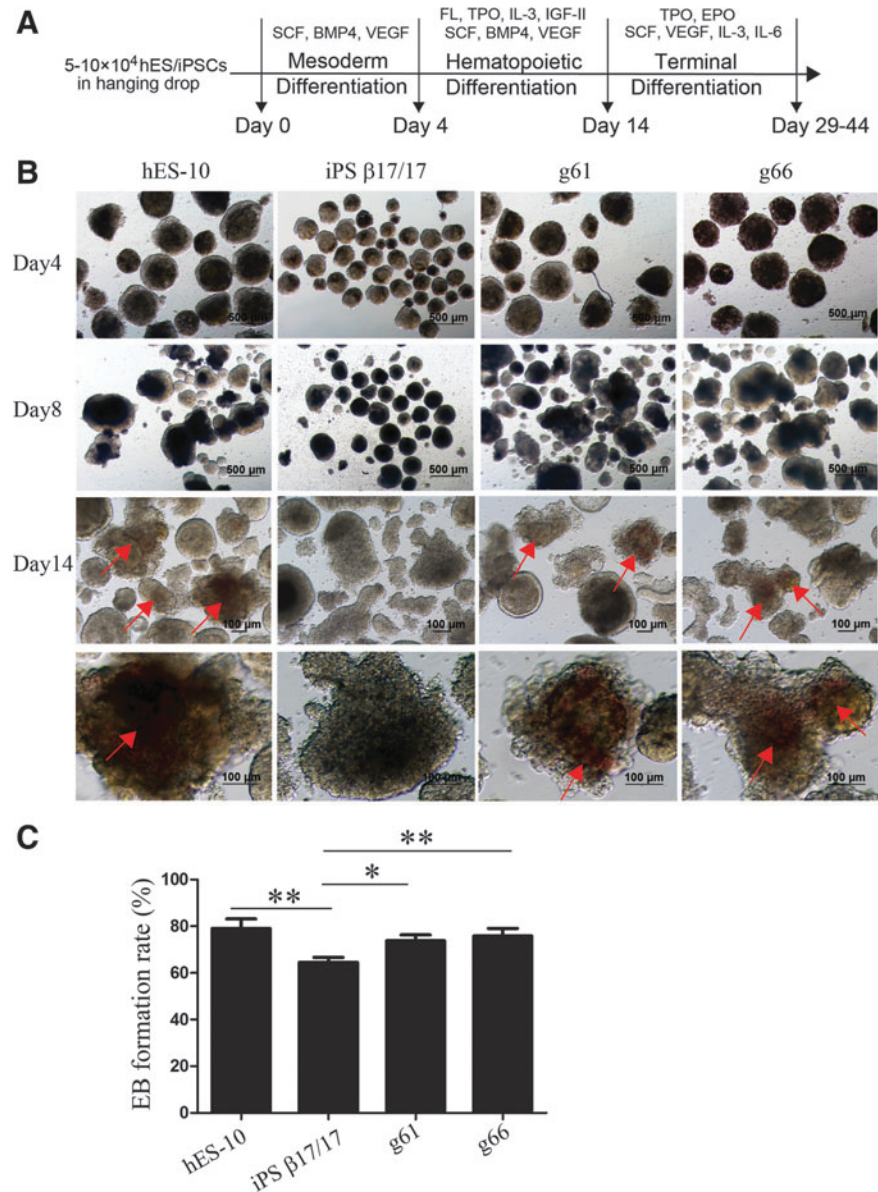
Characterization of the gene-corrected β -Thal iPSCs

iPS- β 17/17 and three gene-corrected clones, g54, g61, and g66, maintained the normal karyotypes (46, XX) (Supplementary Fig. S2A) and retained their pluripotency by expression of ESC markers, such as OCT3/4, SSEA-4, and TRA-1-60 (Supplementary Fig. S2B), and pluripotent genes, such as OCT3/4, SOX2, and NANOG (Supplementary Fig. S2C, D). Two gene-corrected clones, g61 and g66, were used in the following hematopoietic differentiation and they could differentiate into cells of the three germ layers in vitro (Supplementary Fig. S3A) and form teratomas in vivo, containing three germ layers (Supplementary Fig. S3B). Besides, short tandem repeat (STR) analysis was carried out to test 16 different genetic loci in patient fibroblast cells, iPS- β 17/17, and three gene-corrected iPSCs, which showed that all the four iPSC lines had the same origin with the patient fibroblast cells without contamination (Supplementary Table S4).

EB formation ratio and morphologic changes during hematopoietic differentiation

We employed the EB strategy in combination with a chemically defined system to examine the hematopoietic differentiation of hESCs (hES-10), iPS- β 17/17, g61, and g66. The schematic diagram of the protocol for hematopoietic differentiation is shown in Fig. 2A. The differentiation protocol was divided into three sequential stages, including mesoderm induction, hematopoietic stem/progenitor cell emergence, and terminal differentiation. The kinetic change of EB morphology was imaged during the time course of EB formation (Fig. 2B). As time passed, EBs took shape, became larger, and matured. Single, small round cells were also observed to be

FIG. 2. Differences in EB formation ratio and morphology of hES-10, iPS- β 17/17, g61, and g66 cells during the hematopoietic differentiation process. (A) Schematic diagram of the protocol used for hematopoietic differentiation. We employed the EB strategy and a chemically defined system to examine the hematopoietic differentiation of hESCs and iPSCs. This process was divided into three sequential stages: mesoderm induction, hematopoietic stem/progenitor cell emergence, and terminal differentiation. (B) Morphological changes of EBs during differentiation. The photographs of day 14 EBs are listed and red arrows indicate reddish cells most likely belonging to erythroid progenitors. The last row of photographs shows the corresponding higher magnification images of day 14 EBs. (C) Statistical results of the EB formation rate displayed as the mean \pm SD ($n=3$). $**P<0.01$ and $*P<0.05$. BMP4, bone morphogenetic protein 4; EB, embryoid body; EPO, erythropoietin; FL, Flt3 ligand; IGF, insulin-like growth factor; IL, interleukin; SCF, stem cell factor; SD, standard deviation; TPO, thrombopoietin; VEGF, vascular endothelial growth factor.



released from the EBs. The average size of the iPS- β 17/17 EBs was smaller than hES-10, g61, and g66 groups, while there were no obvious differences among the latter three groups. On day 14, reddish cells also appeared in EBs, which most likely belonged to erythroid progenitors. These cells are highlighted with red arrows in Fig. 2B (day 14). The EB formation efficiency of the four groups was $(79.00\% \pm 8.29\%)$, $(64.50\% \pm 4.20\%)$, $(73.75\% \pm 5.06\%)$, and $(75.75\% \pm 6.50\%)$, respectively. The EB formation ratio of iPS- β 17/17 was significantly lower than the other three groups ($P<0.05$, Fig. 2C), but no significant difference was found among the other three groups ($P>0.05$, Fig. 2C). These results demonstrated that the EB formation ratio of gene-corrected iPSCs was improved obviously in comparison with the iPS- β 17/17.

Flow cytometric analysis of various subsets of hematopoietic stem/progenitor cells

Representative flow cytometry plots and their corresponding statistical columns for the four groups are shown

in Fig. 3. The percentages of HSCs ($CD34^+/CD45^+$), hematoendothelial progenitor cells ($CD34^+/CD31^+$), erythroid precursors ($CD34^+/CD71^+$), and erythro-megakaryocytic progenitors ($CD34^+/CD235^+$) from the iPS- β 17/17 group were all lower than the hES-10 group ($P<0.05$, Fig. 3). These differentiation efficiencies were greatly improved in the two gene-corrected groups, g61 and g66, compared with the iPS- β 17/17 group ($P<0.05$, Fig. 3), except for the $CD34^+/CD31^+$ percentage of the g61 group ($P>0.05$, Fig. 3).

Changes of hematopoietic-related genes during differentiation

We harvested day 14 EBs of the four groups, extracted total RNA, and quantified the expression of hematopoietic-related genes. The statistical results are shown in Fig. 4. We found that these genes tested were all higher in the hES-10 group than the iPS- β 17/17 group ($P<0.05$, Fig. 4), except for *HBG* ($P>0.05$, Fig. 4). There was no significant

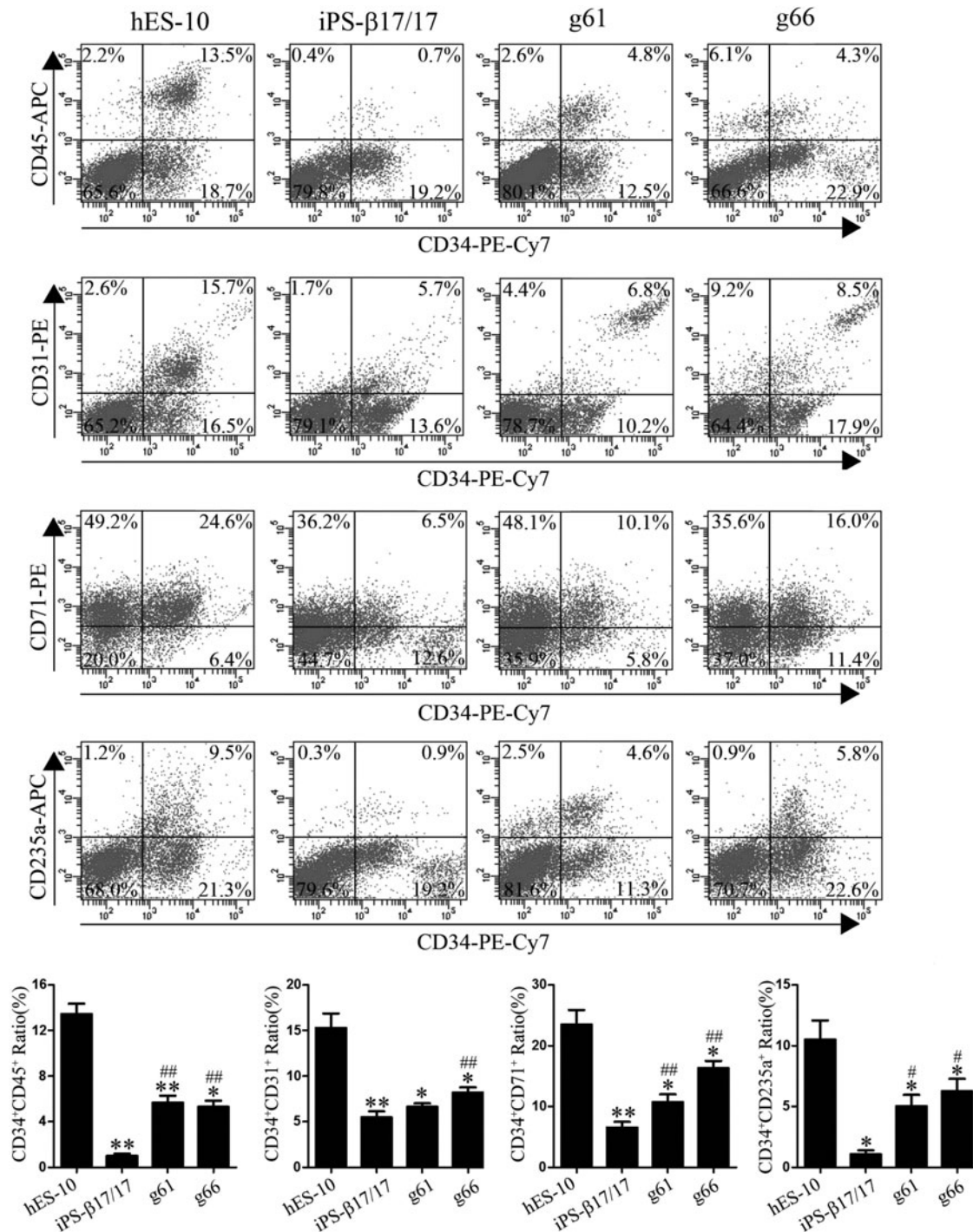


FIG. 3. Flow cytometric analysis of various hematopoietic-related precursors from differentiated hES-10, iPS- β 17/17, g61, and g66 cells. Representative flow cytometry plots of hematopoietic stem and progenitor cells (CD34⁺/CD45⁺), hematoendothelial progenitor cells (CD34⁺/CD31⁺), erythro-megakaryocytic progenitors (CD34⁺/CD235a⁺), and erythroid precursors (CD34⁺/CD71⁺), and statistical results for the four precursors (mean \pm SD, $n=3$) are shown. ** $P < 0.01$ and * $P < 0.05$ compared with the hES-10 group. ### $P < 0.01$ and # $P < 0.05$ compared with the iPS- β 17/17 group.

difference among the four groups in the expressions of *HBG* ($P > 0.05$, Fig. 4). When compared with the expression of lateral mesoderm, marker *FLK1* from gene-corrected g61 and g66 was much lower ($P < 0.05$, Fig. 4), which may be downregulated at the HSC-specific stage. However, the erythroid cell-specific gene, *HBB*, and transcriptional regu-

lators (*GATA-1*, *KLF1*, *RUNX1*, and *FOG1*) from gene-corrected groups were all greatly improved than the iPS- β 17/17 group ($P < 0.05$, Fig. 4). Meanwhile, there was no statistical difference between hES-10 and gene-corrected g61 and g66 in the expression of *CD34*, *CD45*, *ITGA2B*, *KLF*, *RUNX1*, and *FOG1* ($P > 0.05$, Fig. 4).

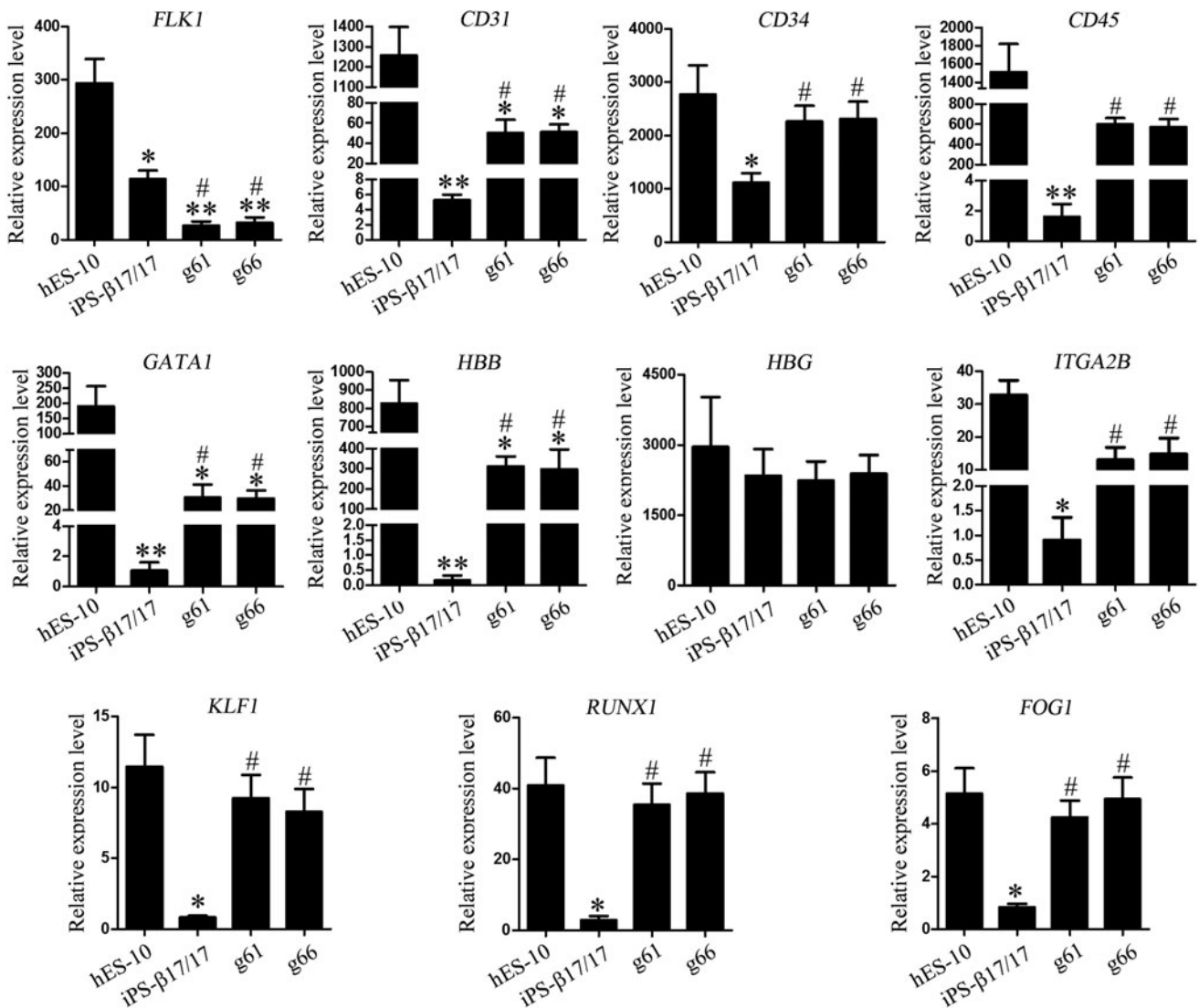


FIG. 4. Evaluation of hematopoiesis-related genes in hES-10, iPS-β17/17, g61, and g66 cells during the differentiation process. RNA was extracted from day 14 EBs, and gene expression was quantified by qRT-PCR. Statistical results of phase-specific genes are shown as the mean ± SD, $n=3$. ** $P<0.01$ and * $P<0.05$ compared with the hES-10 group. # $P<0.05$ compared with the iPS-β17/17 group. *FLK1* is a mesoderm-specific gene. *CD31* expressed in primitive endothelial cells ($CD31^+$) with hemangioblastic properties, which give rise to hematopoietic cells during differentiation. *CD34* and *CD45* are HSC-specific transcription factor genes. *GATA-1* is one of the most important transcription factors in hematopoiesis. β -Globin (*HBB*) and γ -globin (*HBG*) are expressed in hESCs and iPSC-derived erythrocytes. *ITGA2B* is a platelet-related gene. *KLF1*, *RUNX1*, and *FOG1* are important transcriptional regulatory factors in the process of hematopoiesis. HSC, hematopoietic stem cell; iPSC, induced pluripotent stem cell; qRT-PCR, quantitative reverse transcription PCR.

The number and distribution of various CFCs

Hematopoietic colony-forming assays were used to evaluate the hematopoietic differentiation ability of ESCs or iPSCs in vitro. Five lineages of terminally differentiated HSCs (CFC-E, CFC-GEMM, CFC-GM, CFC-G, and CFC-M) were scored when cultured into MethoCult H4434 for another 14 days. From the statistical results, we found that iPS-β17/17-derived HPCs could give rise to various blood lineages, but the numbers were much lower compared with the hES-10 group, especially the erythroid lineage (CFU-E) ($P<0.01$, Fig. 5). The terminal differentiation abilities of gene-corrected iPSCs, g61 and g66, were markedly improved, and the number of CFU-E increased significantly

($P<0.01$, Fig. 5), while there still was a significant statistical difference between the two gene-corrected groups and the hES-10 group ($P<0.01$, Fig. 5).

ROS production, early apoptosis, and proliferation/apoptosis-related gene testing

After 14 days of differentiation, we employed the H_2DCF -DA staining to detect the ROS levels of $CD34^+$ $CD45^+$ HSCs. The representative histogram of FACS and statistical results are shown in Fig. 6A and C, respectively. The levels of ROS from the two gene-corrected groups, g61 and g66, decreased obviously when compared with the iPS-β17/17 group ($P<0.05$, Fig. 6C). However, there was no

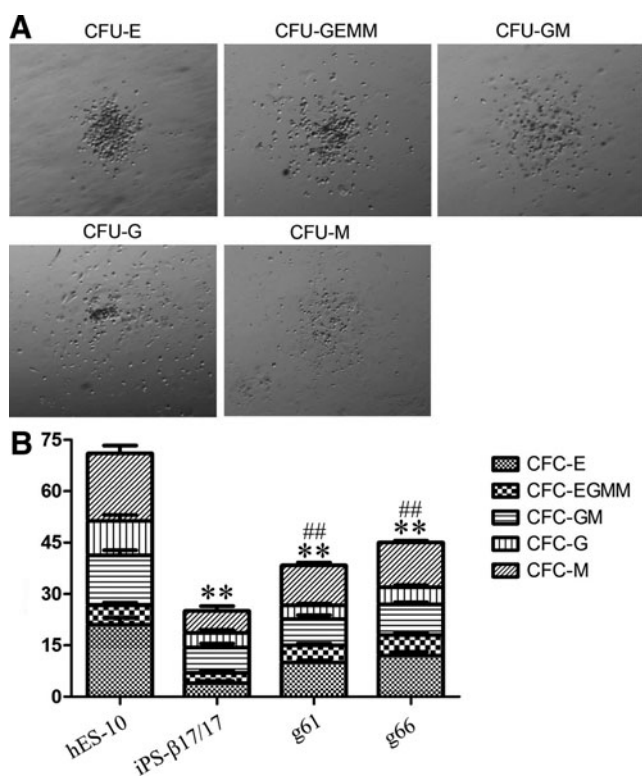


FIG. 5. CFU assays performed on sorted CD34⁺ cells derived from hES-10, iPS-β17/17, g61, and g66 cells. (A) Representative images to show morphology of various hematopoietic CFU populations. Scale bar 500 μm. (B) Cell distribution in CFUs from differentiated hES-10, iPS-β17/17, g61, and g66 cells on day 14. E, erythroid; G, granulocyte; GEMM, granulocyte/erythrocyte/macrophage/megakaryocyte; GM, granulocyte/macrophage; M, macrophage. ** $P < 0.01$ compared to hES-10 group CFC-E number. ### $P < 0.01$ compared to iPS-β17/17 group CFC-E number. CFC, colony-forming cell.

significant difference between the two gene-corrected groups and the hES-10 group ($P > 0.05$, Fig. 6C). Accompanied by the decrease of ROS, the ratios of early apoptotic CD34⁺CD45⁺ HSCs from gene-corrected groups were also significantly reduced compared with the iPS-β17/17 group ($P < 0.05$, Fig. 6D), which still had a statistical difference with the hES-10 group ($P < 0.05$, Fig. 6D). At the gene level, proliferation (*Ki67*, *PCNA*) and apoptosis-related genes (*Caspase-3*) of the gene-corrected group were much lower than the hES-10 group and the iPS-β17/17 group ($P < 0.05$, Fig. 6E–G), while the levels of the antiapoptosis gene, *Bcl-2*, of the gene-corrected groups were elevated visibly compared with the iPS-β17/17 group, which still did not achieve the level of the hES-10 group ($P < 0.05$, Fig. 6H). We speculated that some antiapoptosis mechanisms were activated once the mutation of iPS-β17/17 was corrected by the CRISPR/Cas9 system.

HBB and HBG proteins expression tested by western blotting

To evaluate whether gene-corrected g61 and g66 restored the expression of HBB, we also investigated the levels of

HBB and HBG during hematopoietic differentiation using western blotting. The results indicated that gene-corrected g61 and g66 restored the HBB expression compared with the parental iPSCs ($P < 0.05$, Fig. 7B), which were still lower than the hES-10 group ($P < 0.05$, Fig. 7B). However, HBG levels had no obvious changes among hES-10, iPS-β17/17, and the two gene-corrected lines ($P > 0.05$, Fig. 7C), which was consistent with the transcription results detected by quantitative reverse transcription PCR (qRT-PCR).

Discussion

β-Thal, one of the most common genetic diseases worldwide, has been identified in more than 200 different mutations [26]. In this study, we studied a homozygous point mutation at CD17 (A→T) in HBB, which corrected by the CRISPR/Cas9 system. The genome targeting efficiency directed by sgRNA greatly enhanced compared with traditional homologous recombination [20], and our targeting efficiency was 16.67%. Besides, this system possesses several advantages: simple, easy, and fast when compared with the previous ZFN and TALEN [21]. We have successfully corrected one allele of the mutated HBB genes using our gRNA system by the homologous recombination method. Three gene-corrected lines maintained the normal karyotypes (46, XX) and retained their pluripotency. The gene-editing strategy will relieve the clinical consequences and promote the clinical application of gene-corrected patient-specific iPSCs.

Gene-corrected patient-specific iPSCs provide a stable source for the treatment of genetic and degenerative diseases, which will avoid the high risk of graft rejection to the maximum. However, the hematopoietic differentiation efficiency of gene-corrected β-Thal iPSCs has not been well evaluated [18,19,23]. In the current study, we found that the hematopoietic differentiation ability of gene-corrected iPS-β17/17 by CRISPR/Cas9 was greatly improved with higher hematopoietic progenitor cell percentages, upregulated transcription factor profile, more balanced CFC distribution, and restored HBB expression. Although HBB gene and protein expression restored, which formed the adult hemoglobin (HbA) protein, the fetal hemoglobin (HbF) component, HBG had no significant change, which was consistent with the fact that erythroid precursors from ESCs or iPSCs preferentially express embryonic and HbF, but not HbA [18,23,27,28]. At the same time, it also suggested that globin switches that occur during development need further investigation.

Studies have shown that primitive endothelial cells (CD31⁺) with hemangioblastic properties give rise to hematopoietic cells during differentiation [29,30]. We found that the percentage of CD34⁺CD31⁺ hematoendothelial progenitor cells (HEs) from the iPS-β17/17 group was lower than the gene-corrected groups (Fig. 3). Although the mechanisms regulating the emergence of HSCs from HEs in vivo and in vitro have not been well studied, we speculated that the decrease in HEs may contribute to the poor hematopoietic differentiation ability of β-Thal iPSCs. This ability was obviously improved in cells with the corrected mutation. In addition, the percentages of HSCs (CD34⁺/CD45⁺), erythro-megakaryocytic progenitors (CD34⁺/CD235⁺), and erythroid precursors (CD34⁺/CD71⁺) from

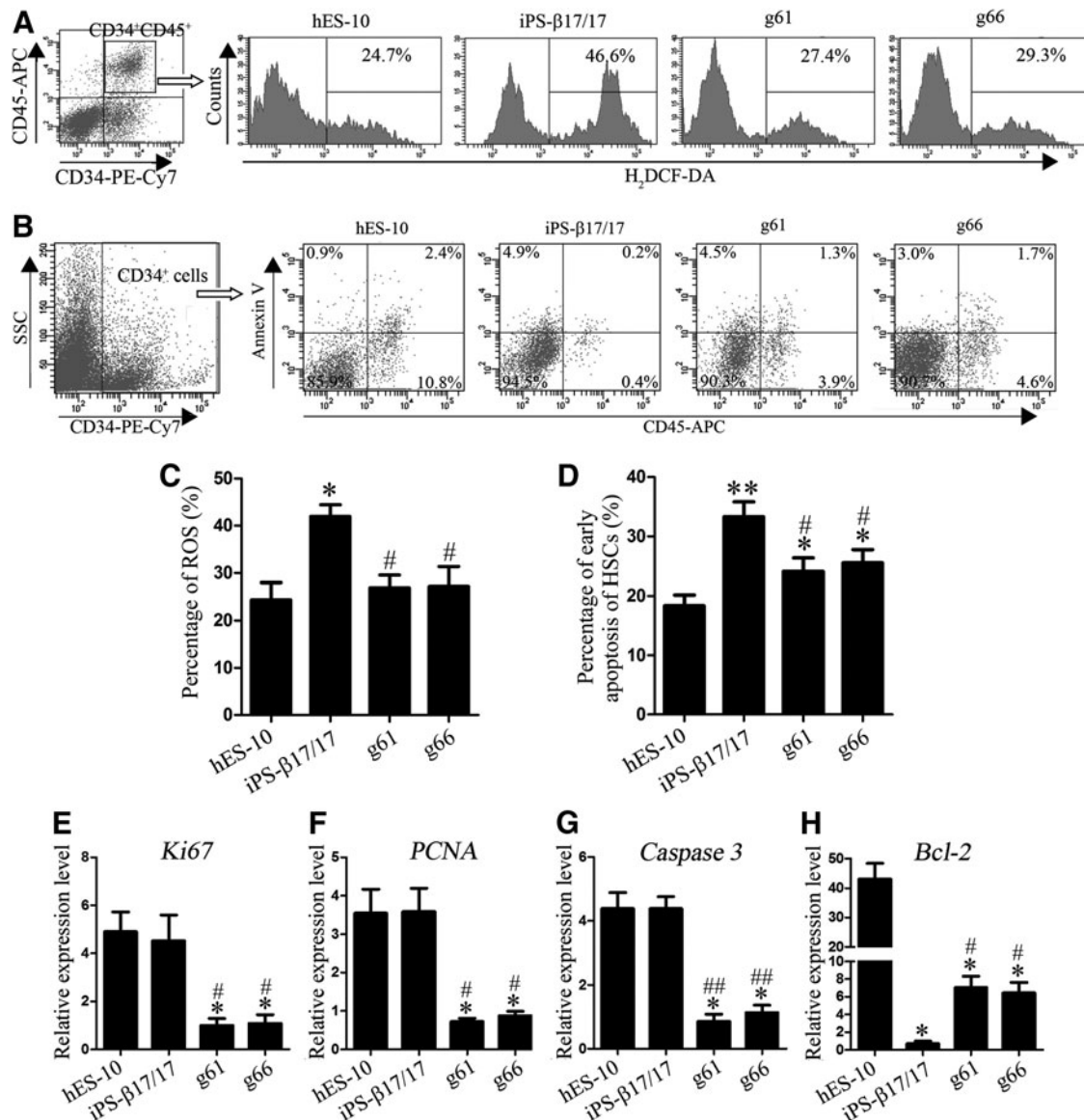


FIG. 6. ROS production, early apoptosis, and proliferation/apoptosis-related gene testing. (A) After 14 days of differentiation, H₂DCF-DA staining and flow cytometry were used to test the ROS production of CD34⁺CD45⁺ HSCs. The representative histogram of FACS is shown in (A), and the statistical results of ROS-positive HSC ratios are presented in (C). (B) The result of early-stage apoptosis of CD34⁺CD45⁺ HSCs stained by Annexin-V is demonstrated by dot plots of FACS in (B), and the corresponding column result is shown in (D). (E–H) At the gene level, proliferation-related genes, *Ki67* and *PCNA*, apoptosis-related gene, *Caspase-3*, and antiapoptosis gene, *Bcl-2*, expression during differentiation were quantified by qRT-PCR, and the results are shown (E–H) accordingly. All statistical results are shown as the mean ± SD, $n=3$. ** $P<0.01$ and * $P<0.05$ compared with the hES-10 group. ## $P<0.01$ and # $P<0.05$ compared with the iPS-β17/17 group. *PCNA*, proliferating cell nuclear antigen; ROS, reactive oxygen species.

the gene-corrected β-Thal iPSC group were also greatly improved, which directly contributed to the elevated hematopoietic differentiation ability and the restoration of HBB expression.

Hematopoiesis is regulated intrinsically, by phase-specific transcription factors and small RNAs, and extrinsically, through growth factors and extracellular matrix secreted by niche cells [31]. *FLK1*, also known as VEGF receptor 2, is a marker of lateral mesoderm [32] and expresses on blood and endothelium progenitors, so-called hemangioblasts [33], which may be downregulated at the HSC-specific stage. So, the lesser expression of *FLK1* in gene-corrected groups may

be beneficial to their further differentiation. *GATA* transcription factors have been shown to play important roles in hematopoiesis. *GATA-1* is the master gene regulating erythropoiesis and positively regulates specific erythroid genes, such as erythropoietin receptor (EPoR), glycophorin (GpA), and globin chains [11], and is also required for megakaryocyte and erythrocyte differentiation [34]. While *FOG1* interaction with *GATA-1* helps maintain erythroid homeostasis and regulates the *HBB* transcription [35,36], *KLF1* directly regulates *HBB* expression and the switching between fetal and adult globin expression [37]. *RUNX1* plays an important role in the development of the

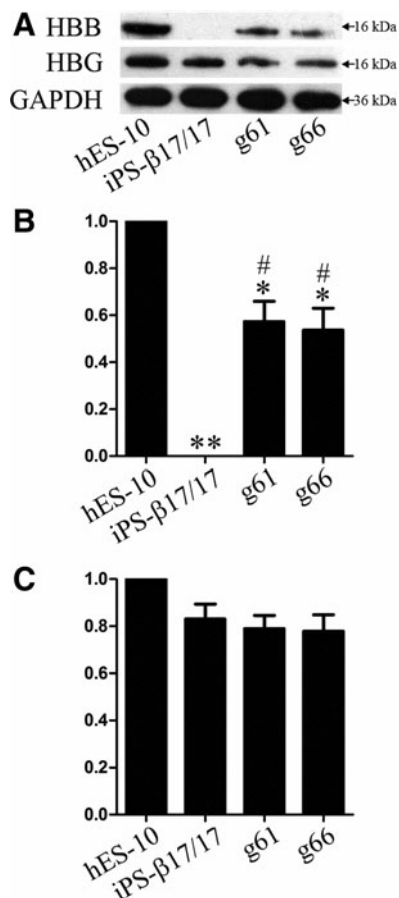


FIG. 7. HBB and HBG proteins detection by western blotting. **(A)** After 14 days of differentiation, total proteins from EBs were separated with 15% SDS-PAGE, transferred to PVDF membrane, and blotted with anti-HBB and anti-HBG Ab. Data are shown in the representative pictures of three independent experiments. **(B)** Density ratios of HBB to GAPDH. **(C)** Density ratios of HBG to GAPDH. All statistical results are presented as the mean \pm SD ($n=3$). ** $P < 0.01$ and * $P < 0.05$ compared with the hES-10 group. # $P < 0.05$ compared with the iPS- β 17/17 group. SDS-PAGE, sodium dodecyl sulfate–polyacrylamide gel electrophoresis.

hematopoietic differentiation, and is crucial for the maturation of HSCs [38]. *ITGA2B* contributes to HSCs and megakaryocyte/platelet functions [39]. From the above, we speculated that upregulated hematopoietic-related transcription factor expression may be another reason for the improved hematopoietic differentiation ability of gene-corrected β -Thal iPSCs.

β -Thal is a hereditary anemic disease, resulting from the unbalanced synthesis of globin chains whereby α -globin chains are in excess. Deposition of the excess α -globin chains is believed to be the origin of several molecular abnormalities in β -Thal erythroid cells, such as IE, oxidative stress (ROS production), and excessive apoptosis [10,11]. IE is characterized by accelerated erythroid differentiation, maturation blockade at the polychromatophilic stage, and death of erythroid precursors [40,41], while enhanced apoptosis was one of the key reasons for IE in human β -Thal [40–42]. We found that the ROS production and the percentage of early-stage apoptotic HSCs of the two gene-corrected

groups reduced significantly compared with uncorrected β -Thal iPSCs, which may improve the IE of β -Thal and explain the improved hematopoietic differentiation ability of gene-corrected β -Thal iPSCs from another aspect. Besides, the proliferation-related gene, *Ki67*, and proliferating cell nuclear antigen (*PCNA*) upregulated in the β -Thal iPSC group compared with gene-corrected groups. Along with the proliferation, the apoptosis-related gene, *Caspase-3*, increased and the antiapoptosis gene, *Bcl-2*, decreased in the β -Thal iPSC group. However, all these changes were reversed in the gene-corrected groups. It is commonly believed that overproliferation will cause apoptosis [43]. So, we speculated that the proliferation of β -Thal iPSCs caused the apoptosis, but did not activate the antiapoptosis mechanism. However, some *Bcl-2*-dependent anti-apoptotic mechanisms were activated in the gene-corrected group with decreased production of ROS and early-stage apoptosis, which improved the hematopoietic differentiation ability and may finally relieve the IE of β -Thal iPSCs.

From this study, our strategy of targeting realized by the CRISPR/Cas9 system had successfully corrected one allele of mutated *HBB* genes without off-targeting and restored the *HBB* gene expression during hematopoietic differentiation. The gene-editing strategy we reported will provide a new pattern of genetic repairing of single-gene inheritance diseases corrected by the CRISPR/Cas9 system. Meanwhile, we also evaluated the hematopoietic differentiation ability of the gene-corrected β -Thal iPSCs. Elevated $CD34^+$ $CD31^+$ HES, upregulated hematopoietic-related transcription factor expression, and some activated antiapoptotic mechanisms may explain the improved hematopoietic differentiation efficiency of the gene-corrected group, which will provide an important step toward clinical application of β -Thal iPSC-derived HSCs in transplantation.

Acknowledgments

The authors thank Professor Yuet Wai Kan and Dr. Lin Ye for providing assistance in the establishment of the hematopoietic differentiation method using the EB strategy. This work was supported by the National Natural Science Foundation-Guangdong Joint Fund (U1132005, 31171229), Science and Information Technology of Guangzhou Key Project (2011Y1-00038, 201400000004), Guangdong Province Higher Education Funding (Yq2013135), General Financial Grant from the China Postdoctoral Science Foundation (2013 M531833 to B.S.), and the Doctoral Foundation from The Third Affiliated Hospital of Guangzhou Medical University, China (2012C63 to B.S.).

Author Disclosure Statement

Each author has nothing to disclose.

References

- Galanello R and R Origa. (2010). Beta-thalassemia. *Orphanet J Rare Dis* 5:11.
- Rivella S and E Rachmilewitz. (2009). Future alternative therapies for β -thalassemia. *Expert Rev Hematol* 2:685.
- Fan Y, Y Luo, X Chen, Q Li and X Sun. (2012). Generation of human β -thalassemia induced pluripotent stem cells from amniotic fluid cells using a single excisable lentiviral stem cell cassette. *J Reprod Dev* 58:404–409.

4. Marziali M, A Isgrò, J Gaziev and G Lucarelli. (2009). Hematopoietic stem cell transplantation in thalassemia and sickle cell disease. Unicenter experience in a multi-ethnic population. *Mediterr J Hematol Infect Dis* 1:e2009027.
5. Cooley TB and P Lee. (1925). A series of cases of splenomegaly in children with anemia and peculiar bone changes. *Trans Am Pediatr Soc* 37:29–30.
6. Weatherall DJ. (2001). Phenotype-genotype relationships in monogenic disease: lessons from the thalassaemias. *Nat Rev Genet* 2:245–255.
7. Thein SL. (2005). Pathophysiology of {beta} thalassemia: a guide to molecular therapies. *Hematology Am Soc Hematol Educ Program* 1:31–37.
8. Libani IV, EC Guy, L Melchiori, R Schiro, P Ramos, L Breda, T Scholzen, A Chadburn, Y Liu, et al. (2008). Decreased differentiation of erythroid cells exacerbates ineffective erythropoiesis in beta-thalassemia. *Blood* 112: 875–885.
9. Tuzmen S and AN Schechter. (2001). Genetic diseases of hemoglobin: diagnostic methods for elucidating beta-thalassemia mutations. *Blood Rev* 15:19–29.
10. Rivella S. (2009). Ineffective erythropoiesis and thalassaemias. *Curr Opin Hematol* 16:187–194.
11. Ribeil JA, JB Arlet, M Dussiot, IC Moura, G Courtois and O Hermine. (2013). Ineffective erythropoiesis in β -thalassemia. *ScientificWorldJournal* 2013:394295.
12. Weatherall DJ. (2010). Thalassemia as a global health problem: recent progress toward its control in the developing countries. *Ann N Y Acad Sci* 1202:17–23.
13. Isgrò A, J Gaziev, P Sodani and G Lucarelli. (2010). Progress in hematopoietic stem cell transplantation as allogeneic cellular gene therapy in thalassemia. *Ann N Y Acad Sci* 1202:149–154.
14. Boulad F, I Rivière and M Sadelain. (2009). Gene therapy for homozygous beta-thalassemia. Is it a reality? *Hemoglobin* 33: S188–S196.
15. Hanna J, M Wernig, S Markoulaki, CW Sun, A Meissner, JP Cassady, C Beard, T Brambrink, LC Wu, TM Townes and R Jaenisch. (2007). Treatment of sickle cell anemia mouse model with iPS cells generated from autologous skin. *Science* 318:1920–1923.
16. Wang Y, Y Jiang, S Liu, X Sun and S Gao. (2009). Generation of induced pluripotent stem cells from human beta-thalassemia fibroblast cells. *Cell Res* 19:1120–1123.
17. Ye L, JC Chang, C Lin, X Sun, J Yu and YW Kan. (2009). Induced pluripotent stem cells offer new approach to therapy in thalassemia and sickle cell anemia and option in prenatal diagnosis in genetic diseases. *Proc Natl Acad Sci U S A* 106:9826–9830.
18. Ma N, B Liao, H Zhang, L Wang, Y Shan, Y Xue, K Huang, S Chen, X Zhou, et al. (2013). Transcription activator-like effector nuclease (TALEN)-mediated gene correction in integration-free β -thalassemia induced pluripotent stem cells. *J Biol Chem* 288:34671–34679.
19. Wang Y, CG Zheng, Y Jiang, J Zhang, J Chen, C Yao, Q Zhao, S Liu, K Chen, et al. (2012). Genetic correction of β -thalassemia patient-specific iPS cells and its use in improving hemoglobin production in irradiated SCID mice. *Cell Res* 22:637–648.
20. Cong L, FA Ran, D Cox, S Lin, R Barretto, N Habib, PD Hsu, X Wu, W Jiang, LA Marraffini and F Zhang. (2013). Multiplex genome engineering using CRISPR/Cas systems. *Science* 339:819–823.
21. Mali P, L Yang, KM Esvelt, J Aach, M Guell, JE DiCarlo, JE Norville and GM Church. (2013). RNA-guided human genome engineering via Cas9. *Science* 339:823–826.
22. Schwank G, BK Koo, V Sasselli, JF Dekkers, I Heo, T Demircan, N Sasaki, S Boymans, E Cuppen, et al. (2013). Functional repair of CFTR by CRISPR/Cas9 in intestinal stem cell organoids of cystic fibrosis patients. *Cell Stem Cell* 13:653–658.
23. Xie F, L Ye, JC Chang, AI Beyer, J Wang, MO Muench and YW Kan. (2014). Seamless gene correction of β -thalassemia mutations in patient-specific iPSCs using CRISPR/Cas9 and piggyBac. *Genome Res* 24:1526–1533.
24. Ye L, MO Muench, N Fusaki, AI Beyer, J Wang, Z Qi, J Yu and YW Kan. (2013). Blood cell-derived induced pluripotent stem cells free of reprogramming factors generated by Sendai viral vectors. *Stem Cells Transl Med* 2:558–566.
25. Fan Y, Y Luo, X Chen and X Sun. (2010). A modified culture medium increases blastocyst formation and the efficiency of human embryonic stem cell derivation from poor-quality embryos. *J Reprod Dev* 56:533–539.
26. Cao A and YW Kan. (2013). The prevention of thalassemia. *Cold Spring Harb Perspect Med* 3: a011775.
27. Chang KH, AM Nelson, H Cao, L Wang, B Nakamoto, CB Ware and T Papayannopoulou. (2006). Definitive-like erythroid from human embryonic stem cells coexpress high levels of embryonic and fetal globins with little or no adult globin. *Blood* 108:1515–1523.
28. Chang KH, A Huang, RK Hirata, PR Wang, DW Russell and T Papayannopoulou. (2010). Globin phenotype of erythroid cells derived from human induced pluripotent stem cells. *Blood* 115:2553–2554.
29. Wang L, L Li, F Shojaei, K Levac, C Cerdan, P Menendez, T Martin, A Rouleau and M Bhatia. (2004). Endothelial and hematopoietic cell fate of human embryonic stem cells originates from primitive endothelium with hemangioblastic properties. *Immunity* 21:31–41.
30. Choi KD, J Yu, K Smuga-Otto, G Salvaggio, W Rehrauer, M Vodyanik, J Thomson and I Slukvin. (2009). Hematopoietic and endothelial differentiation of human induced pluripotent stem cells. *Stem Cells* 27:559–567.
31. Inoue-Yokoo T, K Tani and D Sugiyama. (2013). Mesodermal and hematopoietic differentiation from ES and iPS cells. *Stem Cell Rev* 9:422–434.
32. Kabrun N, HJ Bühring, K Choi, A Ullrich, W Risau and G Keller. (1997). Flk-1 expression defines a population of early embryonic hematopoietic precursors. *Development* 124:2039–2048.
33. Huber TL, V Kouskoff, HJ Fehling, J Palis and G Keller. (2004). Haemangioblast commitment is initiated in the primitive streak of the mouse embryo. *Nature* 432:625–630.
34. Freson K, G Matthijs, C Thys, P Mariën, MF Hoylaerts, J Vermynen and C Van Geet. (2002). Different substitutions at residue D218 of the X-linked transcription factor GATA1 lead to altered clinical severity of macrothrombocytopenia and anemia and are associated with variable skewed X inactivation. *Hum Mol Genet* 11:147–152.
35. Vakoc CR, DL Letting, N Gheldof, T Sawado, MA Bender, M Groudine, MJ Weiss, J Dekker and GA Blobel. (2005). Proximity among distant regulatory elements at the beta-globin locus requires GATA-1 and FOG-1. *Mol Cell* 17:453–462.
36. Hasegawa A, R Shimizu, N Mohandas and M Yamamoto. (2012). Mature erythrocyte membrane homeostasis is

- compromised by loss of the GATA1-FOG1 interaction. *Blood* 119:2615–2623.
37. Satta S, L Perseu, L Maccioni, N Giagu and R Galanello. (2012). Delayed fetal hemoglobin switching in subjects with *KLF1* gene mutation. *Blood Cells Mol Dis* 48:22–24.
 38. Liakhovitskaia A, S Rytsov, T Smith, A Batsivari, N Rytsova, C Rode, M de Bruijn, F Buchholz, S Gordon-Keylock, S Zhao and A Medvinsky. (2014). Runx1 is required for progression of CD41 + embryonic precursors into HSCs but not prior to this. *Development* 141:3319–3323.
 39. Dumon S, DS Walton, G Volpe, N Wilson, E Dassé, W Del Pozzo, JR Landry, B Turner, LP O’Neill, B Göttgens and J Frampton. (2012). Itga2b regulation at the onset of definitive hematopoiesis and commitment to differentiation. *PLoS One* 7: e43300.
 40. Mathias LA, TC Fisher, L Zeng, HJ Meiselman, KI Weinberg, AL Hiti and P Malik. (2000). Ineffective erythropoiesis in beta-thalassemia major is due to apoptosis at the polychromatophilic normoblast stage. *Exp Hematol* 28:1343–1353.
 41. De Franceschi L, M Bertoldi, De L Falco, S Santos Franco, L Ronzoni, F Turrini, A Colancecco, C Camaschella, MD Cappellini and A Iolascon. (2011). Oxidative stress modulates heme synthesis and induces peroxiredoxin-2 as a novel cytoprotective response in β -thalassemic erythropoiesis. *Haematologica* 96:1595–1604.
 42. Centis F, L Tabellini, G Lucarelli, O Buffi, P Tonucci, B Persini, M Annibali, R Emiliani, A Iliescu, et al. (2000). The importance of erythroid expansion in determining the extent of apoptosis in erythroid precursors in patients with beta-thalassemia major. *Blood* 96:3624–3629.
 43. Pal HC, S Sharma, LR Strickland, J Agarwal, M Athar, CA Elmets and F Afaq. (2013). Delphinidin reduces cell proliferation and induces apoptosis of non-small-cell lung cancer cells by targeting EGFR/VEGFR2 signaling pathways. *PLoS One* 8:e77270.

Address correspondence to:

Prof. Xiaofang Sun
Key Laboratory for Major Obstetric Diseases
of Guangdong Province
Key Laboratory of Reproduction and Genetics
of Guangdong Higher Education Institutes
The Third Affiliated Hospital of Guangzhou
Medical University
No. 63 Duobao Road
Liwan District
Guangzhou City 510150
People’s Republic of China

E-mail: xiaofangsun@hotmail.com

Received for publication July 13, 2014

Accepted after revision December 16, 2014

Prepublished on Liebert Instant Online December 17, 2014